

ENGINEERED MATERIALS WITH ANTIBACTERIAL ACTIVITY: Ag AND Pd NANOSTRUCTURES SUPPORTED ON POLYMERS

POLÍVKOVÁ Markéta, SIEGEL Jakub, STASZEK Marek, NOVOTNÁ Zdeňka, ŠVORČÍK Václav

*Department of Solid State Engineering, University of Chemistry and Technology Prague,
Czech Republic, EU, polivko@vscht.cz*

Abstract

Nowadays, biocompatible polymers represent important materials in health-care industry. Their long-term applications, however, lead to the development of infection which must be often suppressed by antibiotic therapy. Resulting problem of resistance of pathogenic bacteria to conventional antibiotics can be effectively solved by antibacterial treatment of polymer-based medical devices. Nanostructured noble metals, such as Ag and Pd, could be advantageously used. We report on antibacterial activity of Ag and Pd nanostructures prepared by DC sputtering on polymeric foils (PI, PEN). Such metal nanolayers of variable thicknesses were transformed by low-temperature post-deposition annealing into discrete nanoislands homogeneously distributed over the underlying polymer. The possibility of managing nanostructure size via controlling the thickness of metal nanolayers prior to the annealing was shown. The surface of engineered metal/polymer composites was characterized and obtained results were discussed with regard to the structural changes induced by annealing process. Antibacterial properties of these composites were evaluated using Gram-positive *Staphylococcus epidermidis* and Gram-negative *Escherichia coli* as model bacterial strains. The way of nanoisland formation and subsequent antibacterial response of prepared metal/polymer composites significantly differs in case of Ag/PI and Pd/PEN, respectively.

Keywords: Polymer, silver, palladium, nanostructures, antibacterial properties

1. INTRODUCTION

Biocompatible polymeric materials exhibit high chemical, mechanical and thermal stability and excellent processability, which, together with their low price, predetermine them to be widespread materials [1]. They are frequently used as the major components of implants, catheters, stents or prostheses [2]. However, it was repeatedly observed that long-term applications of these medical devices can lead to bacterial colonization and biofilm formation resulting in the development of infection, which must be many times treated by antibiotics [3].

Nowadays, healthcare facilities put the emphasis on prevention instead of antibiotic therapy. For this reason, medical devices are often coated by conventional antibiotics [4]. Nevertheless, conventional antibiotics have many disadvantages, including the human cytotoxicity and development of bacterial resistance, which might be primary determined by the type of bacteria, or secondary (acquired) as a result of the bacterial genome evolution. In the view of these disadvantages, non-conventional antibacterial coatings have begun to be investigated. It is well known about silver sulfadiazine that released silver ions inhibit DNA replication of bacteria and deactivate their metabolic enzymes [5]. This knowledge led to examination of nanostructured silver and other noble metals as potential antibacterial coatings [6].

The aim of this work is to reveal the antibacterial activity of Ag and Pd nanolayers, eventually the effect of nanostructures based on these materials, which exhibit high specific surface area. We assume that right the large specific surface area of metal might significantly enhance resulting antibacterial effect. To do so, we prepared Ag- and Pd-based coatings of biocompatible polymers (polyimide, polyethylene naphthalate) frequently used in medical instrumentation, and investigated the antibacterial response of these composites, both before and after annealing. We used two model bacterial strains *Escherichia coli* and *Staphylococcus*

epidermidis, which are frequently involved in hospital-acquired infections associated with a biofilm formation. Surface characterization of these composites was accomplished by the measurement of effective thickness, sheet resistance, and surface morphology. All those parameters were correlated with antibacterial effects.

2. EXPERIMENTAL

2.1. Materials, apparatus and procedures

Polyimide (PI, Kapton HN®, thickness 50 µm, density 1.42 g·cm⁻³), and polyethylene naphthalate foils (PEN, 50 µm, 1.36 g·cm⁻³), supplied by Goodfellow Ltd., UK, were used in this work. The foils were coated by Ag (PI) and Pd (PEN) by diode sputtering system using Balzers SCD 050 device. The metal deposition was accomplished from Ag and Pd targets (purity 99.999 %, Goodfellow Ltd. UK). The parameters of the deposition were: room temperature (20°C), current of 15 mA, total argon pressure of 5 Pa (gas purity 99.99 %), and inter-electrode distance of 50 mm. Sputtering time varied from 10-500 s; samples (\varnothing 2 cm) were prepared during each deposition. Thermal annealing (air, 250°C, and 1 h) was performed immediately after the metal deposition in a thermostat Binder. The annealed samples were then cooled down to room temperature and thereafter stored under standard laboratory conditions.

2.2. Surface characterization methods

Effective thicknesses of Ag and Pd layers were determined on AFM device (see below) by scratch method using Bruker Antimony-doped Silicon probe CONT20A-CP with the spring constant 0.9 N·m⁻¹. Glass substrate, simultaneously coated with polymer samples, was used to measure the thickness of deposited metal. Uncertainty of the measurement was less than 1 %

For the determination of the electrical sheet resistance (R_s) of the metal layers before and after annealing, the standard Ohm's method using KEITHLEY 487 picoampermeter was used. The range of the sputtering times was chosen to cover all of the typical growth stages of the layers (discontinuous, transition area, continuous layer). Two additional metal contacts (about 50 nm thick) were sputtered on the layer surface for R_s measurement. Typical error of the measurement was not exceeding 5 %.

Surface morphology and roughness of pristine and metal-coated samples before and after annealing for various deposition times were examined by AFM using VEECO CP II device working in tapping mode. Surface roughness, characterized by the mean roughness value (R_a), represents the arithmetic average of the deviation from the center plane of the sample.

2.3. Antibacterial tests

Antibacterial properties of pristine and metal-coated polymers (as-sputtered and annealed) were examined by the drop plate method using Gram-negative bacteria *Escherichia coli* (*E. coli*, DBM 3138) and Gram-positive *Staphylococcus epidermidis* (*S. epidermidis*, DBM 3179). *E. coli* was cultivated in Luria-Bertani broth medium (LB) and on LB agar plates, *S. epidermidis* in Plate count broth medium (PCA) and on PCA plates. The inocula were prepared by overnight cultivation in orbital shaker at 37°C. Then, the optical densities were measured at 600 nm.

The starter inocula were prepared by dilution in sterile physiological solution (PS). Tested samples were immersed in 1 ml of PS and inoculated with *E. coli* ($1.1 \cdot 10^4$ of colony forming units (CFU) per 1 ml) and with *S. epidermidis* ($2.2 \cdot 10^4$ of CFU per 1 ml). In parallel, *E. coli* and *S. epidermidis* were incubated solely in PS as positive controls. The samples were incubated at 24°C (*E. coli*) and 37°C (*S. epidermidis*) for 3 h. Aliquots of 25 µl from each sample were placed on pre-dried agar plates in 10-fold repetitions and in a triplicate. After overnight incubation at 24°C (*E. coli*) and 37°C (*S. epidermidis*), the number of CFU was counted. The experiments were accomplished under sterile conditions.

3. RESULTS AND DISCUSSION

3.1. Surface characterization

The effective thicknesses of Ag and Pd nanolayers were examined for the sputtering times of 10-200 s (see **Figure 1**). We found that effective thicknesses of Ag layers exhibited two constant but different deposition rates. The deposition proceeds faster for deposition times of 20-80 s and considerably lower for longer deposition times (100-200 s). Observed transition from faster deposition rate to lower one relates to a transition point between discontinuous and continuous Ag layer (see below R_s), and was also observed for Ag nanolayers on polytetrafluoroethylene [7]. Contrary to that, we found purely linear relationship between the effective thickness of Pd and sputtering time, which indicates strictly proportional sputtering rate.

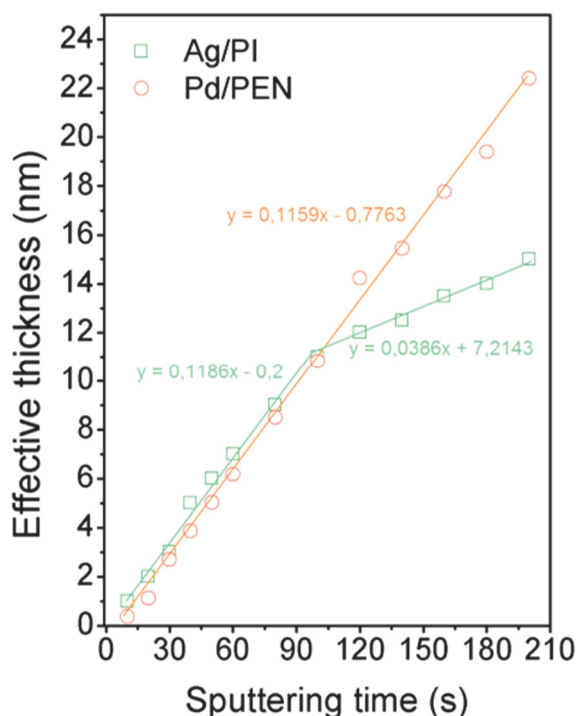


Figure 1 Dependence of the effective thickness of Ag and Pd layers on sputtering time

The measurement of sheet resistance (R_s) was accomplished to examine the electrical continuity of Ag and Pd coatings. One can see the dependence of R_s values on the deposition time of as-sputtered and annealed layers in **Figure 2(a, b)** for Ag/PI and Pd/PEN composites, respectively. It was found that the value of R_s decreased rapidly in the narrow range of the deposition times from 80 to 140 s and from 60 to 140 s for as-sputtered Ag/PI and Pd/PEN, respectively. One can observe that the formation of an electrically continuous metal layer in the case of as-sputtered samples started from the deposition time of 140 s regardless on the specific metal used, while the R_s value was saturated at the level of ca 140 Ω . This is the typical R_s value for nanometer scale metal coatings (Matthiessen's rule) [8]. In the case of annealed samples (both Ag and Pd coated), one can see significant shift of the resistance curve towards longer sputtering times (thicker coatings). This phenomenon is closely related to the changes in the surface morphology observed by AFM (see **Figure 3** below). The annealed metal layers became electrically continuous from the sputtering time of 400 and 160 s, in the case of Pd and Ag layers, respectively; beyond these sputtering times, a percolation limit was overcome and formed layers become continuous from the material point of view. As the sputtering time continued to increase, the R_s value decreased gradually and achieved saturation at the same level, which was observed in the case of the as-sputtered layers.

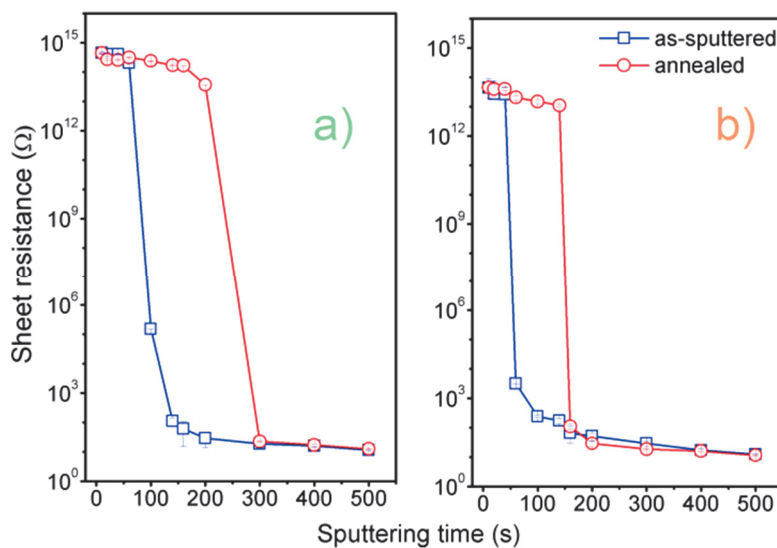


Figure 2 Dependence of the electrical sheet resistance (R_s) on the sputtering time: a) Ag/PI and b) Pd/PEN

Pristine and metal-coated samples of 200 s, both before and after annealing, were studied by AFM to reveal their surface morphology (**Figure 3**) and roughness (R_a) (**Table 1**). The surface morphology of pristine polymers (**Figure 3** left) underwent a soft corrugation during annealing, accompanied by a mild increase of R_a (see **Table 1**). In case of as-sputtered samples, the R_a value remained practically unchanged (mild increase) regardless of specific thickness of metal coating.

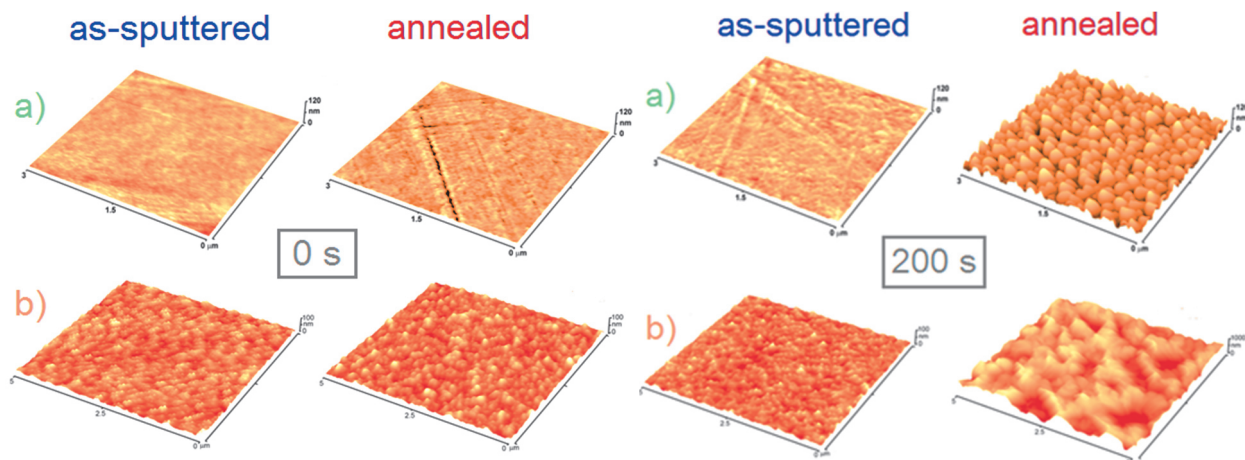


Figure 3 AFM scans of pristine a) PI and b) PEN on the left, and a) Ag/PI and b) Pd/PEN samples of 200 s on the right, before (as-sputtered) and after annealing (annealed)

Remarkable changes in the surface morphology were observed for both Ag/PI and Pd/PEN samples coated for 200 s (**Figure 3** right). One can see that the annealing resulted in the formation of discrete nanoislands, homogeneously distributed over the polymeric surface. Thermally induced changes in the amorphous phase of polymers (transition between the glassy and elastic state) caused that a thicker metal coatings exhibited a thermal accumulation. Enhanced diffusion of metal at elevated temperature led to its aggregation into larger structures. This phenomenon have already been observed in case of Ag [9] and Au [10] nanolayers. These morphology changes were supported by strong increase of R_a (**Table 1**). The R_a was increased by two orders of magnitude for Pd/PEN samples. In case of Ag/PI samples, the increase was less significant; formed Ag

nanoislands were smaller, but more regular. The formation of island-like structures increased the specific surface area of metal.

Table 1 Surface roughness (R_a) of pristine, as-sputtered and annealed Ag/PI and Pd/PEN composites

Samples		Surface roughness (nm)			
		0 s	20 s	100 s	200 s
Ag/PI	as-sputtered	0.6	0.5	1.0	1.7
	annealed	1.0	1.5	2.5	13.8
Pd/PEN	as-sputtered	4.6	4.1	4.4	4.6
	annealed	4.7	4.3	61.7	148.1

Antibacterial effects of Ag/PI and Pd/PEN composites were determined by the drop plate method [11] against two model organisms; *S. epidermidis* and *E. coli* (**Figure 4**). One can see that as-sputtered and annealed Ag-coated PI samples of both deposition times (20 and 200 s) significantly inhibited both bacterial strains. Contrary to that, pristine PI exhibited no antibacterial response in both cases. As expected, the antibacterial effect increased with increasing thickness of Ag layer (increasing sputtering time). Enhanced antibacterial response was observed for annealed samples (both sputtering times) compared to the as-sputtered ones. This effect was presumably caused by expected increase of sample's surface area during annealing (see **Figure 3** right, AFM); the formation of Ag nanoislands. In this connection it should be noted that nature-inspired (on the base of lotus leaf effect) coatings with rough surfaces have been successfully designed for medical applications [12]. Generally, the antibacterial effect of Ag/PI composites had similar trend in case of both bacterial strains.

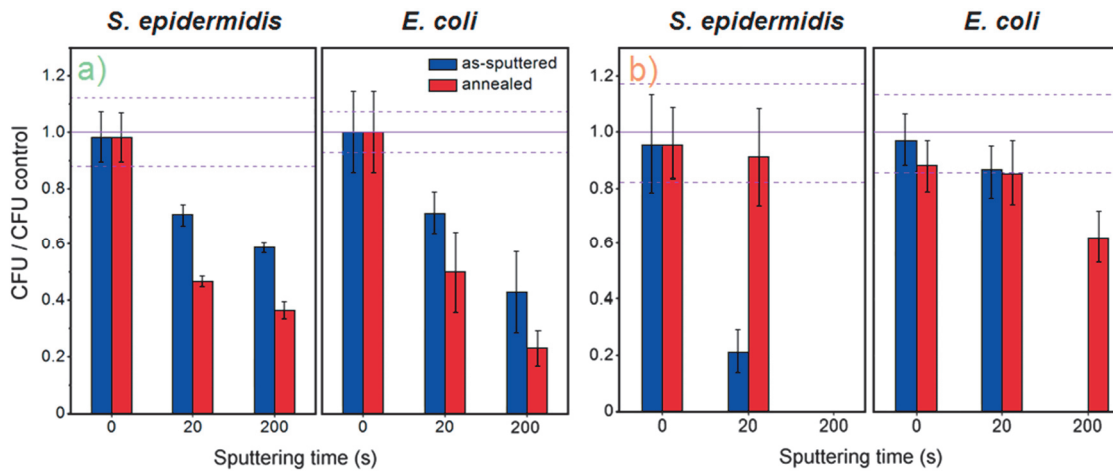


Figure 4 Relative viability (CFU of sample divided by CFU of control) of *S. epidermidis* and *E. coli* for pristine (0 s), as-sputtered and annealed a) Ag-coated and b) Pd-coated samples of the deposition times of 20 and 200 s. Purple line represents reference level (CFU in physiological solution) with its uncertainty (dash lines).

The results for Pd/PEN composites are shown in **Figure 4b**. Similarly as in previous case, pristine polymer exhibited no antibacterial effect (both bacterial strains). Surprisingly, the same trend was observed for the annealed samples of 20 s. Total inhibition effect was determined for both as-sputtered and annealed samples of 200 s in the case of *S. epidermidis*, and for as-sputtered samples in case of *E. coli*. As-sputtered sample of 20 s was also significantly effective against *E. coli*. It is evident, that antibacterial effect increased with increasing sputtering time. However, contrary to Ag/PI, the annealed samples of Pd/PEN were less effective than as-sputtered ones (this finding is in contradiction with the increase of the specific surface area of Pd after annealing). In the light of our other results (XPS, ICP-MS) published elsewhere [13], we attribute the morphology changes not only to the discrete nanoislands, but also to embedding of these clusters into the

polymer interior. This incorporation is very superficial reminding ultrathin (ones of nm) polymer overlay reaching almost the top of individual Pd-islands (for more details see ref. [13] "curtain effect").

4. CONCLUSION

This paper presents an effective way for preparation of metal coatings on polymers, potentially applicable in antibacterial treatment of polymeric medical devices. The surface characterization of these metal/polymer composites was successfully accomplished by diverse methods. The antibacterial efficacy of prepared Ag and Pd coatings was thoroughly tested. It was found that these novel structures are promising materials enable to fight against broad spectrum of microorganisms. We believe that our results provide a good basis for the application of these engineered materials in medicinal technology. Nevertheless, to provide further insight into their safe applications, cytocompatibility testing of these structures must be followed.

ACKNOWLEDGEMENTS

Financial support from specific university research (MSMT No 20-SVV/2016) and GACR under the project No. 14-18131S is gratefully acknowledged.

REFERENCES

- [1] DERSH, R., STEINHART, M., BOUDRIOT, U., GREINER, A., WENDORFF, J.H. Nanoprocessing of polymers: applications in medicine, sensors, catalysis, photonics. *Polymers for Advanced Technologies*, 2005, vol. 16, no. 2-3, pp. 276-282.
- [2] LEWIS, A.L., TOLHURST, L.A., STRATFORD, P.W. Analysis of a phosphorylcholine-based polymer coating on a coronary stent pre- and post-implantation. *Biomaterials*, 2002, vol. 23, no. 7, pp. 1697-1706.
- [3] GAYNES, R., EDWARDS, J.R. Overview of nosocomial infections caused by gram-negative bacilli. *Clinical Infectious Diseases*, 2005, vol. 41, no. 6, pp. 848-854.
- [4] DE NARDO, L., FARE, S., DI MATTEO, V., CIPOLLA, E., SAINO, E., VISA, L., SPEZIALE, P., TANZI, M.C. New heparinizable modified poly(carbonate urethane) surfaces diminishing bacterial colonization. *Journal of Materials Science: Materials in Medicine*, 2007, vol. 18, no. 11, pp. 2109-2115.
- [5] FRANCOLINI, I., DONELLI, G., STOODLEY, P. Polymer designs to control biofilm growth on medical devices. *Reviews in Environmental Science and Bio/Technology*, 2003, vol. 2, no. 2, pp. 307-319.
- [6] RAI, M., YADAV, A., GADE, A. Silver nanoparticles as a new generation of antimicrobials. *Biotechnology Advances*, 2009, vol. 27, no. 1, pp. 76-83.
- [7] SIEGEL, J., JUŘÍK, P., KOLSKÁ, Z., ŠVORČÍK, V. Annealing of silver nanolayers sputtered on polytetrafluoroethylene. *Surface and Interface Analysis*, 2013, vol. 45, no. 6, pp. 1063-1066.
- [8] CHOPRA, K.L. *Thin Film Phenomena*. New York: McGraw Hill, 1969. 127 p.
- [9] OH, Y.J., JEONG, K.H. Glass Nanopillar Arrays with Nanogap-Rich Silver Nanoislands for Highly Intense Surface Enhanced Raman Scattering. *Advanced Materials*, 2012, vol. 24, no. 17, pp. 2234-2237.
- [10] PISCOPIELLO, E., TAPFER, L., ANTISARI, M.V., PAIANO, P., PRETE, P., LOVERGINE, N. Formation of epitaxial gold nanoislands on (100) silicon. *Physical Review B*, 2008, vol. 78, no. 3, 035305.
- [11] CHEN, CH.Y., CHIANG, CH.L. How to optimize the drop plate method for enumerating bacteria, *Materials Letters*, 2001, vol. 44, no. 2, pp. 121-129.
- [12] YANG, H., YOU, W., SHEN, Q., WANG, X., SHENG, J., CHENG, D. Preparation of lotus-leaf-like antibacterial film based on mesoporous silica microcapsule-supported Ag nanoparticles. *RSC Advances*, 2014, vol. 4, no. 6, pp. 2793- 2796.
- [13] POLÍVKOVÁ, M., VALOVÁ, M., SIEGEL, J., RIMPELOVÁ, S., HUBÁČEK, T., LYUTAKOV, O., ŠVORČÍK, V. Antibacterial properties of palladium nanostructures sputtered on polyethylene naphthalate. *RSC Advances*, 2015, vol. 5, no. 90, pp. 73767-73774.